Journal of Mechanical Engineering and Sciences
ISSN (Print): 2289-4659; e-ISSN: 2231-8380
Volume 13, Issue 3, pp. 5259-5277, September 2019

DOI: https://doi.org/10.15282/jmes.13.3.2019.04.0430

Modelling and control of a Magneto-Rheological elastomer for impact reduction

Mohd Sabirin Rahmat[1], Khisbullah Hudha[1*], Zulkiffli Abd Kadir[1], Nur Rashid Mat Nuri[2], Noor Hafizah Amer[1] and Shohaimi Abdullah[3]

[1]Department of Mechanical Engineering, Faculty of Engineering,
National Defence University of Malaysia, Kem Sg. Besi, 57000 Kuala Lumpur, Malaysia
[*]Email: k.hudha@upnm.edu.my
[2]Department of Mechanical Engineering Technology,
Faculty of Engineering Technology,
Universiti Teknikal Malaysia Melaka, Hang Tuah Jaya, 76100 Melaka, Malaysia
[3]Vice Chancellor Management Office, Widad University College, BIM Point Bandar Indera Mahkota, 25200 Kuantan, Pahang Darul Makmur

ABSTRACT

This article presents a simulation analysis of the effectiveness of an impact reduction control-based magneto-rheological elastomer isolator device (MREID). The MREID is an impact isolator device that produces variable stiffness controlled by an input current supply to the device coil. In order to control the input current for the MREID, a hybrid control structure combining the skyhook strategy and active force control strategy is proposed. Firstly, the characteristics of the MREID in squeeze mode were investigated systematically to establish the relationship between the supply input current to the subsequent force and the impact energy within the MREID. The proposed control strategy was used for force tracking control in determining the amount of input current to be applied to the MREID. The desired input current was determined by a current generator that was developed using the inverse ANFIS technique, this generator regulated the amount of input current based on the desired force and impact energy. The effectiveness of the actively controlled MREID was evaluated using MATLAB simulations by comparing the performance of the MREID controlled by skyhook control against a passive damper. It was found that the proposed controller recorded better response compared to the skyhook controller, thus improving the stability and effectiveness of controlling the MREID.

Keywords: Hybrid control; skyhook control; active force control; MRE control strategy; impact reduction control.

INTRODUCTION

Magneto-rheological elastomer (MRE) is a material with rheological properties that can be controlled by regulating the magnetic field within the material. MRE is mainly composed of rubber and micron-sized carbonyl iron particles that form a chain-like structure. By applying external electrical input current to the iron particles, an electromagnetic field can be created, simultaneously introducing variable resistance among the chain-like particles. Changing the supplied current will manipulate the resistance, overall stiffness, and damping properties of the material. This process enables the construction of a controllable elastomeric component suitable for vibrational and impact isolators, as well as for controllable suspension systems.

Therefore, in order to enhance the performance of an MRE device for any application, mathematical modelling to predict the actual behaviour of the MRE device and development of a control strategy both play important roles. This is because prediction through simulation analysis enables rapid development of the MRE device by evaluating its performance with a control strategy. In recent studies of MREs, most researchers have discussed their modelling technique for cyclic loading and vibration applications, but impact loading applications are less commonly discussed. Since the modelling method is important for the development of control strategies, and MRE devices possess non-linearity behaviour, hysteresis properties and uncertainty properties as stated in [1–8], modelling MRE device behaviour for impact loading is challenging. Many modelling methods have been proposed to predict MRE device behaviour, including the viscoelastic model, Kelvin–Voigt model, Bingham model, adaptive neuro-fuzzy inference system (ANFIS) and polynomial approach. In this study, the ANFIS model is selected to predict MRE device behaviour, because this method provides a relatively low percentage of relative error and provided fast modelling technique.

Since MRE is still relatively new in the smart material family, publications on MRE control are currently limited in number. Previously, the mechanical properties for MRE were controlled by varying an applied magnetic field [9–13]. Previous works have proposed controlling mechanical properties such as vibration, shock or impact for different applications of the isolation system. Therefore, the control strategies that have been used for MRE materials and devices include fuzzy logic control (FLC) [14,15], ON–OFF control [16–18] and semi-active control [19–22], in order to increase the MRE's effects and achieve optimum performance for the devices. Jie Fu et al. [15] introduced a new semi-active control strategy using FLC to control the variable stiffness of the MRE. These authors reported that the acceleration transmissibility was reduced by 54% while using the proposed controller, compared to that achieved while using passive and ON–OFF control. Yang et al. [23] studied an MRE isolator with a negative changing stiffness to reduce vibration by designing a hybrid magnet system consisting of positive and negative current to the MRE device.

Motivated by recent studies, the goals of the work presented in this paper were to develop an MRE isolator device (MREID) model using ANFIS and to develop a control strategy for the MREID. In this study, the design of the MREID for impact loading application was developed, and characterization of the MREID was conducted using an impact pendulum test rig. Then, the data obtained from this characterization work was processed and used to train the ANFIS model in predicting the MREID's behaviour. The modelling method presented in this study was a fast modelling method with a minimum relative error compared with experimental data. Next, a controller was designed, namely a hybrid of skyhook and active force control (HYSAFC), to produce the desired amount of input current to the MREID coils. The development of the proposed control strategy was intended to improve on the performance of the skyhook controller in eliminating unwanted impact energy to the plant system. Additionally, the plant system for the control structure to evaluate control performance, a dynamic model of a shock isolator system based on a single-degree-of-freedom (SDOF) setup, was developed, and the performance criteria for evaluating the controller characteristics namely jerk, acceleration and force were used in this study.

This paper is organised as follows: The first section contains a brief introduction and summary of previous developments in control strategies for MRE. The second section presents the modelling of the MREID, followed by a description of the proposed control strategy for the MREID for impact loading applications in the third section. The fourth section elaborates on the experimental setup, which was designed to measure the behaviour of the MREID. The fifth section discusses the simulation results to evaluate the effectiveness of the control strategy. Finally, the last section presents the conclusions of this study.

MAGNETO-RHEOLOGICAL ELASTOMER ISOLATOR DEVICE

Design of a Magneto-Rheological Elastomer Isolator Device

Figures 1(a) and 1(b) show a cross-sectional view and external design, respectively, of the MREID. The MREID consists of six different geometrical components, namely the shaft sleeve, strut, primary coil, secondary coil, MRE solid and MRE layer. The shaft sleeve, strut, primary and secondary coils bobbin was fabricated using magnetic field material namely low carbon steel 1020. The primary coil consists of 300 wire turns, while the secondary coil contains 150 wire turns. The two coils are designed to generate a magnetic field for the MRE solid and MRE layer, respectively. The working operating mode for the proposed MREID design is squeeze mode; the advantage of including two layers of MRE material is to increase the damping force in squeeze mode.

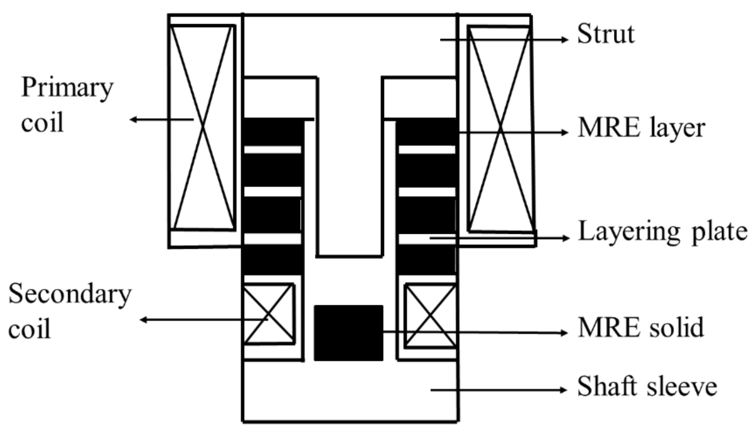

Figure 1(a). Cross-sectional view of the MREID design.

Fabrication of MRE Material

In order to develop the MREID, room temperature vulcanizing silicone rubber (produced by Craftivity Malaysia) and silicone oil were selected as the matrix. The weight ratio of the silicone rubber and the silicone oil in the composition matrix was 1:1. Carbonyl iron particles with a 5 µm diameter (Sigma-Alrich, USA) were used to produce variable stiffness when applying different magnetic fields. These particles were mixed in with the silicone rubber and silicone oil. The mixture was stirred for ten minutes and then poured into a mould, which was inserted into a vacuum case for 30 minutes to remove the air bubbles. No magnetic field was applied during the curing process, which lasted about 24 hours. The weight of physical MRE samples was measured to be 10 g.

Figure 1(b). Physical structure of the MREID.

Magnetic Circuit Analysis of Proposed MREID

An electromagnetic analysis is one of the important aspects to consider in designing an MRE isolator. To analyse the distribution of the magnetic flux, Finite Element Method Magnetics software was used. In order to evaluate the magnetic field at maximum input current to the coil device, a two-dimensional cross-section of the device was created, as depicted in Figure 2. The MREID is divided into three components. The first component is the shaft sleeve and strut, while the second component is the MRE layer and solid MRE structures. The layer structure consisted of four layers of MRE material with a thickness of 5 mm, and each layer was fixed to a stiffening plate, which was made of magnetic material. Meanwhile, the solid MRE material was located inside the shaft sleeve. The third component is referred to as the coil bobbin, in which two sets of coils were used to generate a better MRE effect for the layer and solid. The primary and secondary coils both used a wire gauge of 24 AWG.

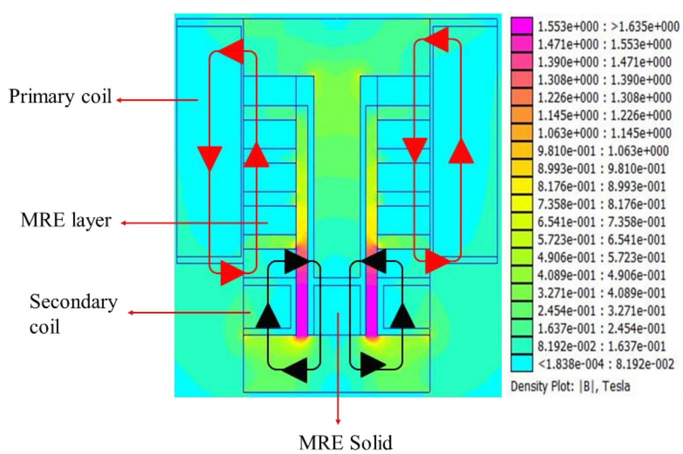

Figure 2. Magnetic intensity for MRE isolator device.

From the above figure, it can be seen that the distribution of magnetic flux passes through the isolator for a maximum input current of 3 amperes are 0.9 T and 1.5 T for the MRE layer and MRE solid, respectively. In this analysis, the result at 3 amperes is presented because the device produces its maximum magnetic intensity at the maximum input current. Based on the results of this analysis, it was demonstrated that the properties of the MRE in this MREID are properly influenced by the input current.

CHARACTERIZATION OF MAGNETO-RHEOLOGICAL ISOLATOR DEVICE

The characteristics of the MREID were analysed by measuring the dynamic behaviour using an impact pendulum test rig with various impact energies and input currents. A detailed procedure for conducting this experiment was provided by [24]. Next, the data obtained from this procedure was used to plot the data in the form of force–displacement and force–velocity characteristics. Through the plotted results, each impact energy was represented by hysteresis loops from 0 to 3 amperes of input currents with 0.5 ampere increments. The force–displacement and force–velocity characteristics from the hysteresis loops are shown in Figure 3 and Figure 4, respectively.

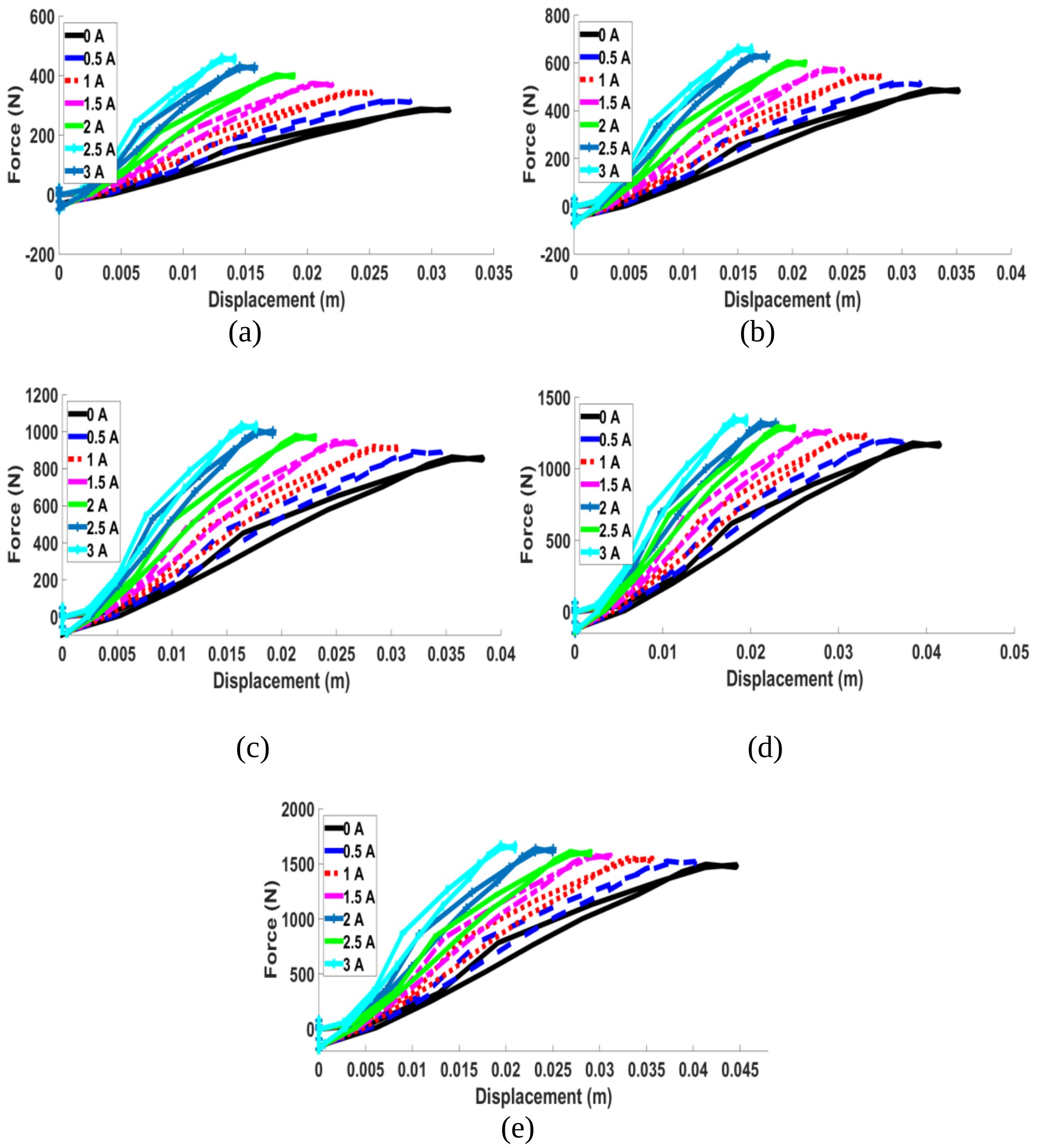

Figure 3. Force versus displacement characteristic for MREID, (a) 10.81 J, (b) 32.43 J, (c) 54.06 J, (d) 75.68 J and (e) 97.30.

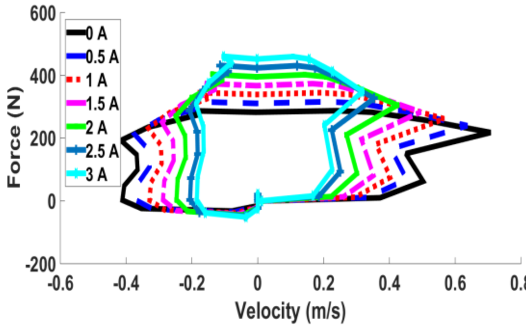

(a)

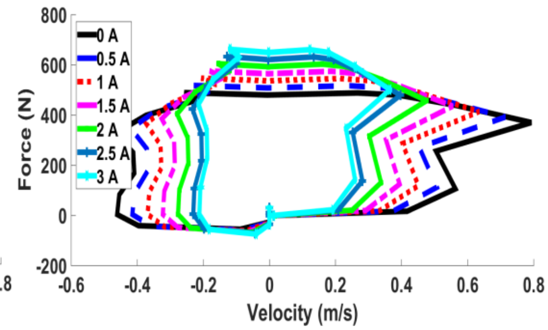

(b)

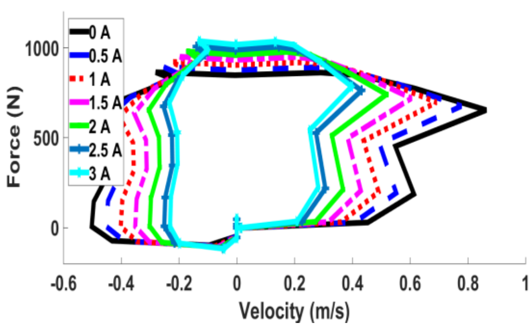

(c)

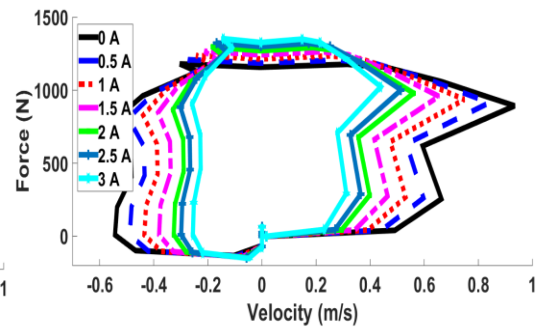

(d)

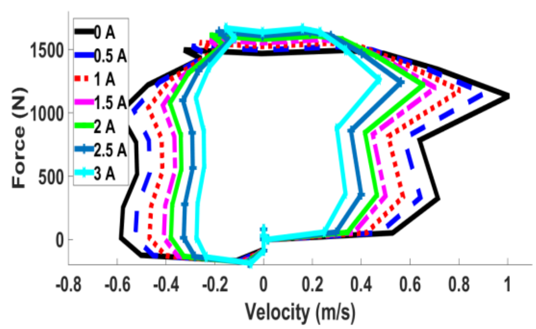

(e)

Figure 4. Force versus velocity characteristic for MREID, (a) 10.81 J, (b) 32.43 J, (c) 54.06 J, (d) 75.68 J and (e) 97.30.

From Figures 3 and 4, it can be seen that force increased proportionally when the input current was increased. Meanwhile, the displacement and velocity decreased when the input current was increased. These results demonstrate that the MREID can be used as a variable stiffness device for a controllable impact isolator. The trend of hysteresis loops results was shown to trend consistently upward when input current applied to the MREID coils increased. Moreover, it can be seen that the ability of the MRE material to produce a damping force of 3 amperes for 10.81 J was significant. However, for 97.30 J, the performance of MRE material at 3 amperes was not significantly different than that seen at 2.5 amperes. Yet the damping force still increased, even though this increase was not significant. These results fall into an acceptable range to suggest that the device can be used as an impact isolator.

MODELLING OF MAGNETO-RHEOLOGICAL ISOLATOR DEVICE UNDER IMPACT LOADING

Based on the previously reported characteristics of the MREID, the data obtained from the experiment was used to train using an interpolated multiple ANFIS approach to predict MREID behaviour under impact loading. In the training ANFIS model, there were three pieces of input data (piston velocity of the isolator, input current to the MREID coil and impact energy produced by pendulum mass) and a single desired output (impact force absorbed by the MREID) used to load the data into the ANFIS toolbox in MATLAB Simulink software. The ANFIS architecture is shown in Figure 5.

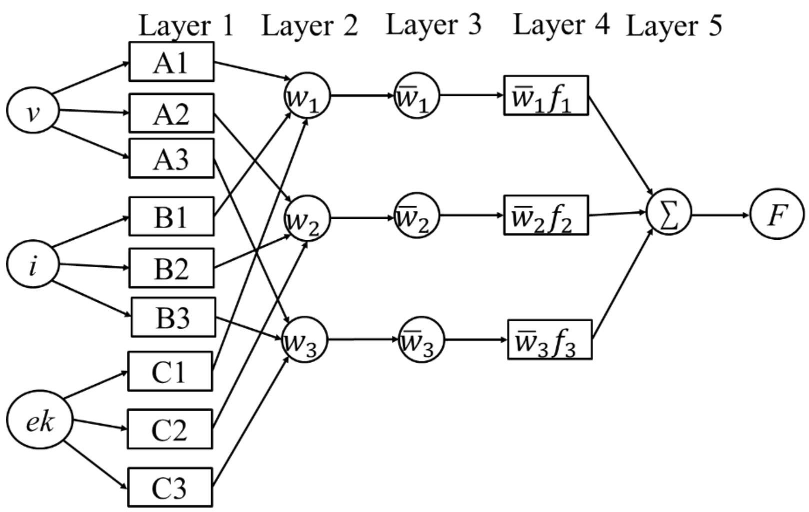

Figure 5. ANFIS architecture.

In Figure 5, a circle indicates a fixed node, whereas a square indicates an adaptive node. For an ANFIS, the three fuzzy IF–THEN rules based on the first-order Sugeno model are considered as follows:

Rule (1): IF *v* is A1 AND *i* is B1 AND *ek* is C1 THEN $f_1 = p_1 d + q_1 i + r_1 ek + t_1$

Rule (2): IF *v* is A2 AND *i* is B2 AND *ek* is C2 THEN $f_2 = p_2 d + q_2 i + r_2 ek + t_2$

Rule (3): IF *v* is A3 AND *i* is B3 AND *ek* is C3 THEN $f_3 = p_3 d + q_3 i + r_3 ek + t_3$

where:
v, *i* and *ek* are the inputs;
A_i, B_i and C_i are the fuzzy sets;
fi is the output within the fuzzy region specified by the fuzzy rule;
p_i, q_i, r_i and t_i are the design parameters that were determined during the training process.

In training the neural network, there were forward pass and backward pass methods. At each layer, in turn, for the forward pass method, the algorithm used the least square method to identify the consequent parameter in layer 1 until layer 4. The operations of each layer in the ANFIS architecture can be described as follows.

Layer 1: Every node, *i*, in this layer is a square node with a node function

$$O_i^1 = \mu_{A_i}(d) \tag{1}$$

The output O_i^1 denotes the membership degree of the *i*-th mode of the first layer. μ is the membership function of the fuzzy set A_i. Normally, the function $\mu_{A_i}(d)$ is defined based on the shape of the membership function to be used. In this case, the bell-shaped Gaussian membership function was chosen, and the function can be defined as:

$$\mu_{Ai}(d) = \exp^{-\left(\frac{(d-x)^2}{2\cdot\sigma^2}\right)} \tag{2}$$

where *x* and σ are the centre and spread of the Gaussian function, respectively. As the values of these parameters change, the Gaussian function varies accordingly.

Layer 2: Each node in this layer is a circular node with its output defined as the product of all input signals. For any *i*-th node, the node's output (ω_i), which also defines the firing strength of a rule, is defined as follows:

$$\omega_i = \mu_{A_i}(d) \times \mu_{B_i}(i) \times \mu_{Ci}(ek) \quad i = 1,2\ldots. \tag{3}$$

Layer 3: Each node in this layer is a fixed node. The *i*-th node calculates the ratio between the firing strength of the *i*-th rule and the sum of all firing strengths.

$$O_{3,i} = \bar{\omega}_i = \frac{\omega_i}{\omega_1 + \omega_2 + \omega_3} \quad i = 1,2\ldots. \tag{4}$$

The output from this layer is defined as the normalised firing strength.

Layer 4: The *i*-th node in this layer represents an adaptive node with output function

$$O_{4,i} = \bar{\omega}_i f_1 = \bar{\omega}_i (p_i d + q_i i + r_i ek + t_i) \tag{5}$$

where $\bar{\omega}_i$ is the normalised firing strength from layer 3, while p_i, q_i and t_i are the parameters set in this layer, and these are referred to as the consequent parameters.

Layer 5: The single node for this layer is a fixed node; this node computes the overall output through the summation of all the incoming signals from layer 4 nodes:

$$O_{5,1} = \sum_i \bar{\omega}_i f_i = \frac{\sum_i \omega_i f_i}{\sum_i \omega_i} \tag{6}$$

The parameters of the ANFIS data training for subtractive clustering are listed in Table 1. From the data listed, the range of influence and squash factor values were determined through a trial-and-error method.

Table 1. ANFIS Parameters.

Subtractive clustering	
Parameter	Value
Range of Influence	0.0003
Squash factor	0.002
Accept ratio	0.5
Reject ratio	0.15
Epochs	30
Error tolerance	0
Optimised method	hybrid

MODEL OF IMPACT ISOLATION SYSTEM

An impact isolation system model consisting of the semi-active MREID is shown in Figure 6. The impact isolation system was developed based on an SDOF system. The impact energy input produced by the impact force is transmitted to the movable plate. For simplification of the dynamic modelling, it was assumed that only the horizontal motion of the impact isolation system existed. Additionally, the proposed MREID impact isolation system consisted of both MREID and SDOF structure. The MREID was modelled using the ANFIS technique. The SDOF was modelled by a set of linear spring and dampers that produce constant characteristics. Thus, the equation of motion of the impact isolation system can be formulated as follows:

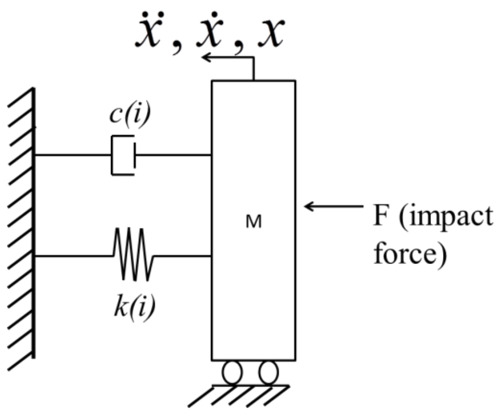

Figure 6. SDOF of impact isolation system.

According to Newton's second law, the dynamic model can be derived as:

$$M\ddot{x} + k(i)x + c(i)\dot{x} = F_{impact} \tag{7}$$

In this model, the mass, *M*, is connected to the fixed wall through MRE device, *MRE* and damping, *c*. Since the characteristics of the MREID produce variable stiffness through adjustment of the input current, the damping properties of the MREID were considered. This is because the damping properties contribute to the absorption of the impact force as well as the isolator, which produces a small damping coefficient effect.

CONTROL STRATEGY

To ensure an efficient controllability for MRE in absorbing the impact force, a controller was developed, aimed at reducing impact energy. For any impact occurrence, the controller determined the amount of damping force required to reduce the impact by supplying the desired amount of input current to the coils. In order to provide the accurate amount of input current, a pre-processing algorithm, namely the current generator, was developed. This algorithm was developed using the inverse ANFIS technique. Then, a proposed control strategy for impact rejection control, HYSAFC, was designed. These two control strategies were combined to improve the stability of the impact dynamic system by considering the system's acceleration. In order to examine the performance of the controller, an SDOF impact isolation system model was developed to evaluate the performance and effectiveness of the proposed controller in reducing impact. Figure 7 shows the SDOF of the impact dynamic system for the MREID considered in this study.

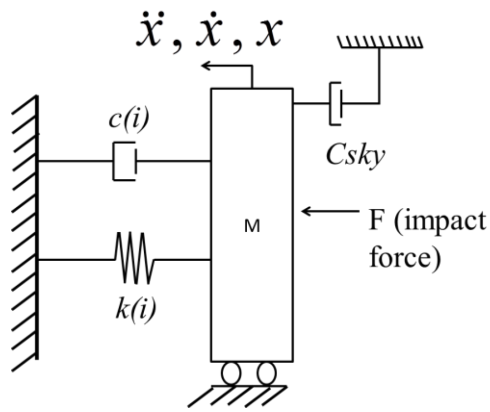

Figure 7. Schematic diagram of impact isolation for the proposed control strategy.

Skyhook Controller

Generally, skyhook control is one of the most popular control strategies in a semi-active suspension system for disturbance rejection control and dynamic system stability improvements [25,26]. In the skyhook control system, an imaginary damper is virtually placed between the movable mass and a fictitious stationary sky to eliminate the motion of the movable mass when the dynamic system is subjected to impact force. The general equation for skyhook control can be described as:

$$F = -C_{sky} \dot{x} \quad (8)$$

where C_{sky}, $\dot{x}$ and F represent the skyhook damping, body velocity and force from control algorithm, respectively.

Active Force Control

Active force control (AFC) was introduced by [27]. The AFC is an effective way to eliminate external disturbance due to the reduced complexity of its control algorithm. Thus, it can be performed on the physical measurement or on the estimated parameters [28–33], the latter of which is easier to implement in real-time applications. The control algorithm for the AFC scheme in obtaining the estimated impact force in the AFC loop is as follows:

$$F_e = \frac{1}{K}(F_a - E_m \cdot \ddot{x}) \tag{9}$$

Here F_e, F_a , E_m and $\ddot{x}$ denote the desired force, actuator force, estimated mass and body acceleration, respectively. These two controllers are combined into the hybrid control strategy for controlling the MRE on an SDOF impact dynamic system. The control structure configuration of the hybrid control strategy is shown in Figure 8.

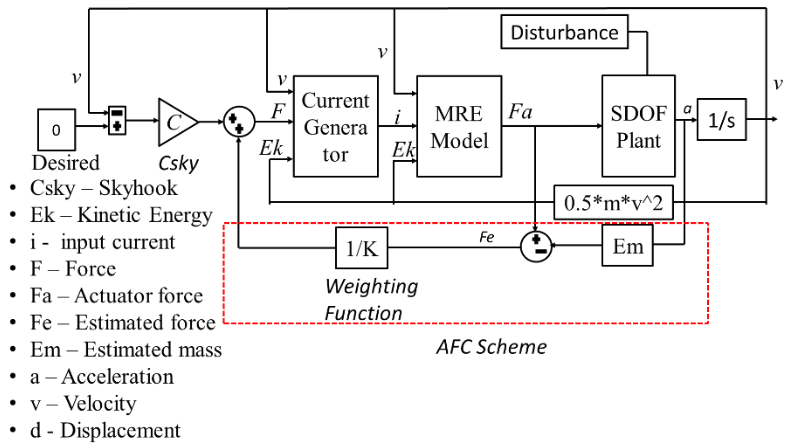

Figure 8. Control structure of the hybrid control.

In the control strategy, the actual velocity of the SDOF impact isolation system was fed back and compared with the desired velocity. The resulting error was scaled using the proportional gain, (C_{sky}). The actual force of the SDOF impact isolation system was obtained by multiplying acceleration and proportional gain, (E_m), and the resulting value was compared with the force actuator, (F_a), to determine the resulting error of estimation force, (F_e). The estimation force, (F_e), was used to scale using a proportional gain weighting function, (K). The equivalent was combined with the proportional gain, (C_{sky}), to provide the control signal to the current generator.

Current Generator

In this study, the current generator was developed as a data pre-processing algorithm to estimate the desired amount of input currents to the MREID coil based on the body velocity of the impact isolation system, impact energy and damping force. In order to estimate the desired amount of input currents, the inverse ANFIS model was used. Based on Figure 6 in the current generator block diagram, the damping force was used as the input of the current generator, and the signal of the force was sent from the controller. However, other inputs, namely impact energy and velocity, were obtained from the calculation of the formula in Figure 6 and the first-order integral of the acceleration impact isolation system. Through the developed model of the current generator, the input currents supplied to the MREID coils could be estimated accurately, and the unwanted impact energy could be eliminated. Here, the suitable input current was selected through a data pre-processing algorithm as follows:

$$i = \left\{ \begin{array}{lll} if & F < 2300N = Low\ \ kinetic\ \ energy, & then \quad i = 1,2,3 \\ if & 2300N <= F < 3500N = Medium\ \ kinetic\ \ energy, & then \quad i = 1,2,3 \\ if & F > 4200N = High\ \ kinetic\ \ energy, & then \quad i = 1,2,3 \end{array} \right\}$$

RESULTS AND DISCUSSION

This section describes the control characteristics and MREID performance with the proposed controller. The MREID performance with the proposed controller was evaluated in terms of jerk, acceleration and force of the SDOF impact isolation system, respectively. In order to analyse the performance of the MREID with the control strategy in simulation, the square shape of impact force was set as the input and the three different impact forces—namely low, medium and high impact energies—were used in a simulation model for this analysis. These analyses were conducted to evaluate the effectiveness of the proposed controller in eliminating various impact energies. The response time of the square shape input was started at 7.2 s to 7.7 s. In the simulation results, the MREID with the proposed controller, skyhook control and passive damper system under low impact energy were compared, and the MREID's performance is presented in Figures 9(a) to 9(c).

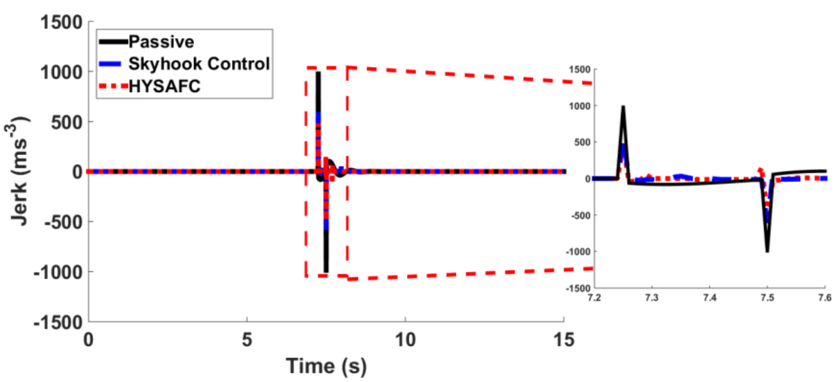

(a)

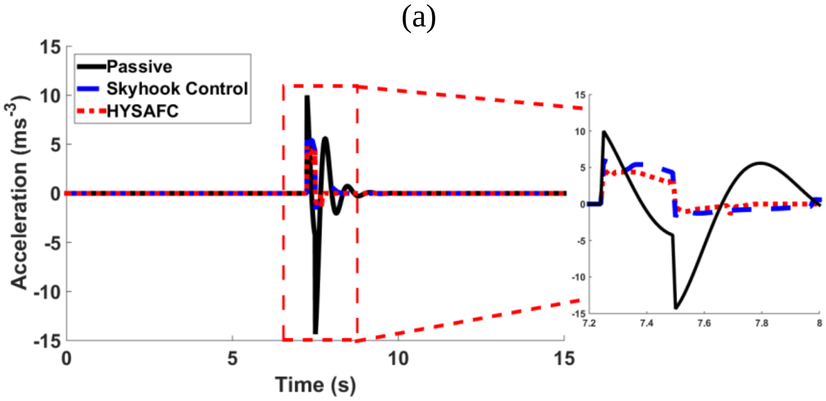

(b)

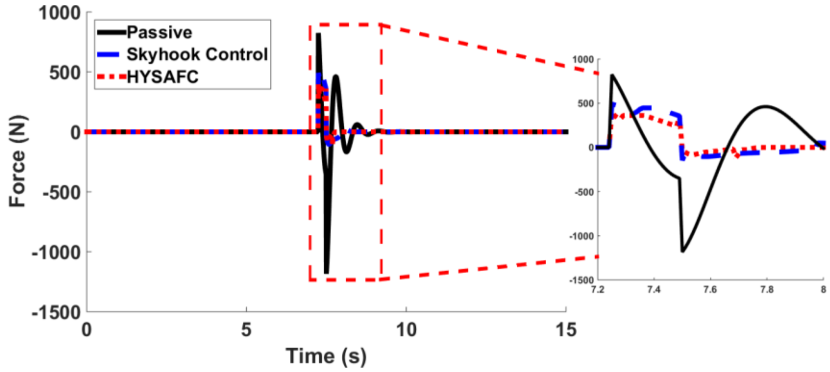

(c)

Figure 9. Simulation result of case analysis 1, (a) jerk versus time, (b) acceleration versus time and (c) force versus time.

The results show that the proposed controller with the tracking control strategy was able to enhance the stability of the impact isolation system. Accordingly, the performance of the hybrid controller was capable of reducing jerk, acceleration and force by 40% compared to that of the passive damper and by 15% compared to that of the skyhook control. The result of the proposed controller performance was also analysed through the root-mean-square (RMS) value, as listed in Table 2.

Table 2. RMS Value for Low Impact Energy Performance.

Performance Criteria	RMS values				
	Passive	Skyhook Control	Percentage Decrease (%)	HYSAFC	Percentage Decrease (%)
Jerk	0.0249	0.0211	15.22	0.0148	40.56
Acceleration	0.1263	0.1070	15.28	0.0749	40.70
Force	0.0380	0.0322	15.24	0.0225	40.81

As shown in the above table, the performance of the proposed controller shows a better performance than that of the skyhook control. For jerk response, the HYSAFC showed an improvement of 40.56%, while the acceleration and force of the impact isolation system were enhanced by 40.70 and 40.81%, respectively. The effectiveness of the proposed controller at assessing the capability of the MREID performance under medium impact energy is shown in Figures 10(a) to 10(c). The performance criteria of jerk, acceleration and force of impact isolation system are also considered in this analysis, to ensure consistency of the proposed controller with different impact energies.

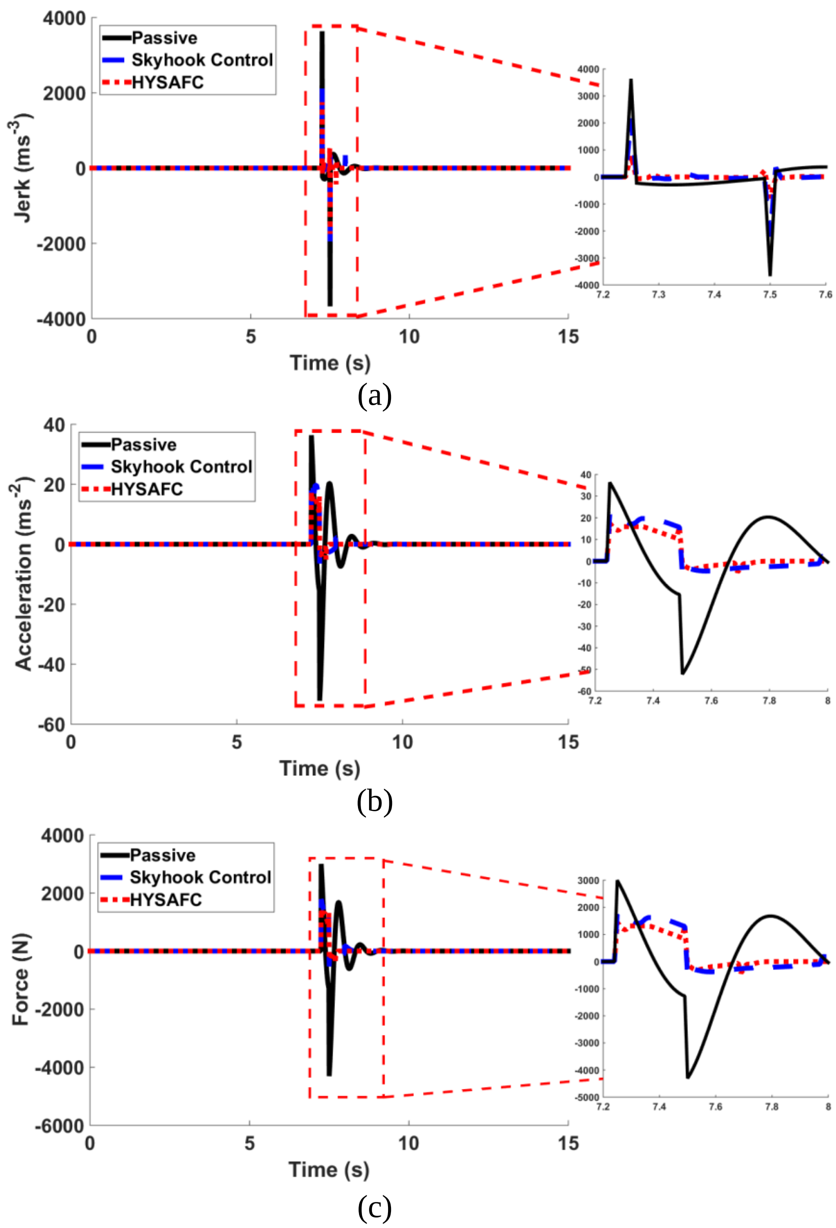

Figure 10. Simulation results of case analysis 2, (a) jerk versus time, (b) acceleration versus time and (c) force versus time.

The results show the performance of the MREID with hybrid control, skyhook control and passive damper systems, evaluated in terms of jerk, acceleration and force of impact isolation under medium kinetic energy. It can be seen from the results that the performance of the proposed controller was reduced by 41% compared with the passive damper system for jerk, acceleration and force of the impact isolation system. The MREID with proposed controller indicated improvement in all the performance criteria under medium impact as compared to low impact energy. Based on the amount of reduction by the MREID, it is clear that the isolator has a better isolation effect than by the alternate controller methods. In the detailed analysis for the proposed controller, the performance of the proposed controller to produce the amount of input current to increase the damping force of the MREID through RMS values is summarized in Table 3.

Table 3. RMS Values for Medium Impact Energy.

Performance Criteria	RMS values				
	Passive	Skyhook Control	Percentage Decrease (%)	HYSAFC	Percentage Decrease (%)
Jerk	0.0918	0.0768	16.34	0.0537	41.50
Acceleration	0.4674	0.3900	16.56	0.2730	41.59
Force	0.0644	0.0536	16.71	0.0375	41.71

The data in Table 3 shows the proportion of different performance in terms of RMS values for the passive damper system and MREID. In this analysis, the MREID with skyhook control and hybrid control were compared with the passive system in terms of RMS values. Based on the summarized data, the jerk response was decreased by 16.34%, while acceleration and force response of the impact isolation system were reduced by 16.56% and 16.71%, respectively, for the MREID controlled by skyhook control. Meanwhile, the hybrid controller indicated promising results in improving the stability of the impact isolation system through the response of jerk, acceleration and force. Figures 11(a) to 11(c) illustrate the performance of the MREID with control strategy under high impact energy in the simulation analysis.

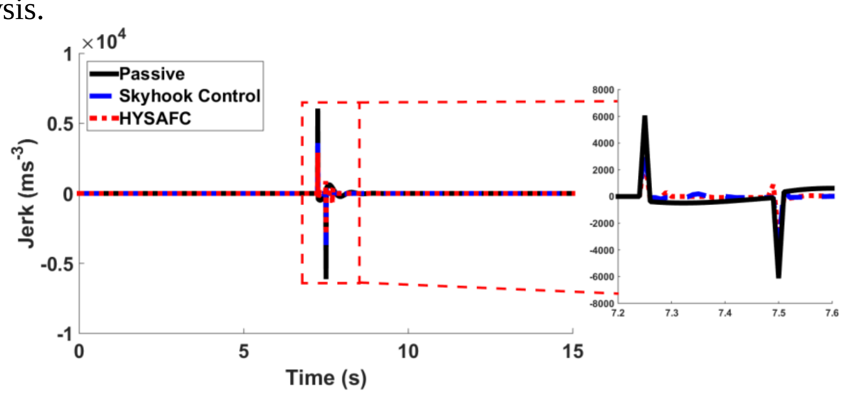

(a)

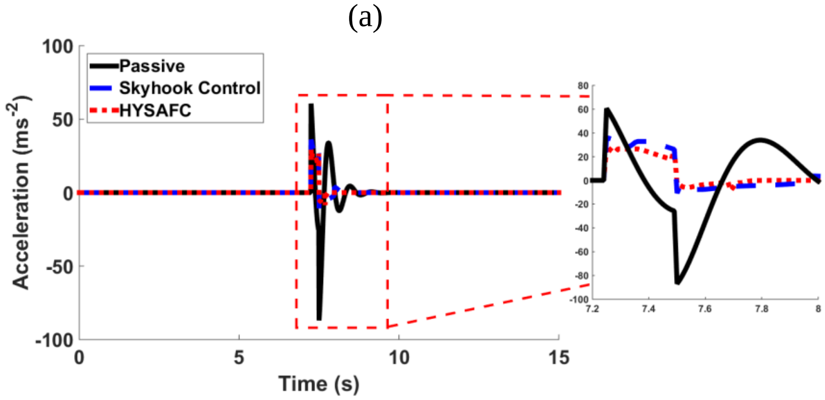

(b)

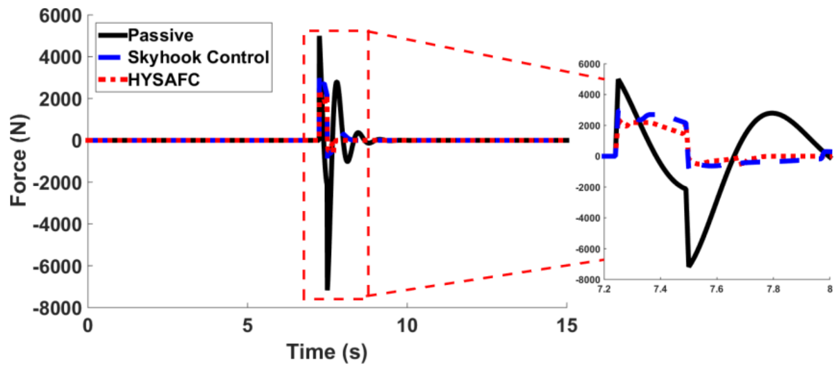

(c)

Figure 11. Simulation results of case analysis 3, (a) jerk versus time, (b) acceleration versus time and (c) force versus time.

It can be seen from the results above that the MREID with proposed controller was successfully dissipated under high impact energy. Based on these results, by comparing the effect on control strategy of MREID performance under low, medium and high impact energies, the hybrid control demonstrated promising results for all performance criteria and cases. The hybrid controller's performance indicated that, when the impact isolation system received higher impact energy, the hybrid controller was capable of producing more damping force in order to attenuate any impact energy. The performance of the proposed controller showed better performance than skyhook control and the quantitative data through RMS values is listed in Table 4. Through this results, the hybrid control demonstrated improvement of 43.14% for jerk response, while the acceleration and force of the impact isolation system were improved by 43.48% and 43.65%, respectively.

Table 4. RMS Values for High Impact Energy

Performance Criteria	RMS values				
	Passive	Skyhook Control	Percentage Decrease (%)	HYSAFC	Percentage Decrease (%)
Jerk	0.1553	0.1280	17.56	0.0883	43.14
Acceleration	0.7911	0.6500	17.84	0.4471	43.48
Force	0.1080	0.0886	17.93	0.0608	43.65

Overall, the performance of the hybrid control showed better results, and jerk, acceleration and force were all reduced by 43% compared to the passive damper. The development of hybrid control was suitable for the MREID design, and facilitated attenuation of unwanted impact energy in the impact isolation system. In future work, the developed hybrid controller will be implemented and tested in real applications using the hardware-in-the-loop-simulation method.

CONCLUSION

In the current study, the effectiveness of impact reduction control for an MREID was performed and simulated using MATLAB Simulink software. The characteristics of the MREID for impact loading was performed using an impact pendulum test rig, and the data obtained from the experimental work was used to model MREID behaviour using the ANFIS technique. The impact isolation system model to represent the plant of the system in the control structure was formulated and also modelled in MATLAB Simulink software. The control strategy algorithm of hybrid control for MREID-based skyhook control and active force control was formulated. Meanwhile, the hybrid control was able to produce an accurate applied current through the current generator. The current generator was modelled using the inverse ANFIS technique to provide the desired amount of input current through a pre-data processing algorithm in the current generator. The simulation results show that the proposed control strategy for MREID was able to attenuate impact energy in any form of energy to the impact isolation. The ability of the proposed controller to effectively adjust the damping force of the MREID during impact was quantified in terms of an improvement in the performance criteria of impact isolation system by 44% for all cases.

ACKNOWLEDGEMENT

This work is supported by the National Defence University of Malaysia (Centre of Research and Innovation Management) and the Ministry of Higher Education of Malaysia through a My PhD scholarship and financial support under the Long-term Research Grant Scheme (L.R.G.S.) with project number LRGS/B-U/2013/UPNM/DEFENSE & SECURITY-P1, led by Associate Professor Dr. Khisbullah Hudha. This financial support is gratefully acknowledged.

REFERENCES

[1] Li Y, Li J, Tian T, Li W. Corrigendum: A highly adjustable magnetorheological elastomer base isolator for applications of real-time adaptive control. Smart Materials and Structures. 2014;23:1-20.

[2] Li Y, Li J, Li W, Du H. A state-of-the-art review on magnetorheological elastomer devices. Smart Materials and Structures. 2014;23:1-24.

[3] Fu J, Yu M, Dong XM, Zhu LX. Magnetorheological elastomer and its application on impact buffer. Journal of Physics: Conference Series. 2013;412:1-10.

[4] Fu J, Li P, Wang Y, Liao G, Yu M. Model-free fuzzy control of a magnetorheological elastomer vibration isolation system: Analysis and experimental evaluation. Smart Materials and Structures. 2016;25:1-13.

[5] Behrooz M, Wang X, Gordaninejad F. Performance of a new magnetorheological elastomer isolation system. Smart Materials and Structures. 2014;23:1–8.

[6] Ubaidillah, Imaduddin F, Li Y, Mazlan SA, Sutrisno J, Koga T, Yahya I, Choi SB. A new class magnetorheological elastomers based on waste tire rubber and properties characterization. Smart Materials and Structures. 2016;25:1–15.

[7] Ubaidillah, Mazlan SA, Sutrisno J, Yahya I, Harjana, Imaduddin F. Physicochemical

properties and stress-strain compression behaviors of a ground tire rubber based magnetorheological elastomers. Scientia Iranica C. 2016;23:1144–59.
[8] Ubaidillah, Choi HJ, Mazlan SA, Imaduddin F, Harjana. Fabrication and viscoelastic characteristics of waste tire rubber based magnetorheological elastomer. Smart Materials and Structures. 2016;25:1-14.
[9] Choi SB, Li W, Yu M, Du H, Fu J, Do PX. State of the art of control schemes for smart systems featuring magneto-rheological materials. Smart Materials and Structures. 2016;25:1-67.
[10] Li Y, Li J, Li W, Samali B. Development and characterization of a magnetorheological elastomer based adaptive seismic isolator. Smart Materials and Structures. 2013;22:1-12.
[11] Carlson JD, Jolly MR. MR fluid, foam and elastomer devices. Mechatronics. 2000;10:555–69.
[12] Chen L, Gong XL. Damping of magnetorheological elastomers. Journal of Central South University of Technology. 2008;15:271–4.
[13] Li WH, Zhang XZ. A study of the magnetorheological effect of bimodal particle based magnetorheological elastomers. Smart Materials and Structures. 2010;19:1–9.
[14] Nguyen XB, Komatsuzaki T, Iwata Y. Fuzzy Semiactive Vibration Control of Structures Using Magnetorheological Elastomer. Shock and Vibration. 2017;2017:1–15.
[15] Fu J, Li P, Wang Y, Liao G, Yu M. Model-free fuzzy control of a magnetorheological elastomer vibration isolation system: Analysis and experimental evaluation. Smart Materials and Structures. 2016;25:1–13.
[16] Ni YQ, Ying ZG, Chen ZH. Magneto-rheological elastomer (MRE) based composite structures for micro-vibration control. Earthquake Engineering and Engineering Vibration. 2010;9:345–56.
[17] Zhu W, Rui XT. Semiactive vibration control using a magnetorheological damper and a magnetorheological elastomer based on the bouc-wen model. Shock and Vibration. 2014;2014:1-10.
[18] Gu X, Yu Y, Li J, Li Y. Semi-active control of magnetorheological elastomer base isolation system utilising learning-based inverse model. Journal of Sound and Vibration. 2017;406:346–62.
[19] Behrooz M, Wang X, Gordaninejad F. Performance of a new magnetorheological elastomer isolation system. Smart Materials and Structures. 2014;23:1-8.
[20] Opie S, Yim W. Design and control of a real-time variable modulus vibration isolator. Journal of Intelligent Material Systems and Structures. 2011;22:113–25.
[21] Opie S, Yim W. Design and control of a real-time variable modulus vibration isolator. IEEE/ASME International Conference on Advanced Intelligent Mechatronics. 2009:380–5.
[22] Zheng J, Li Z, Koo J-H, Wang J. Analysis and compensation methods for time delays in an impact buffer system based on magnetorheological dampers. Journal of Intelligent Material Systems and Structures. 2015;26:690–700.
[23] Yang J, Du H, Li W, Li Y, Li J, Sun S, et al. Experimental study and modeling of a novel magnetorheological elastomer isolator. Smart Materials and Structures. 2013;22:1–14.
[24] Rahmat MS, Hudha K, Kadir ZA, Nuri NRM, Abdullah NHAS. Characterization and

Modelling of a Magneto-Rheological Elastomer Isolator Device under Impact Loadings using Interpolated Multiple Adaptive Neuro Fuzzy Inference System Structure. International Journal of Material and Structural Integrity. 2018:In press.

[25] Amer NH, Ramli R, Mahadi WNL, Abidin MAZ. A review on control strategies for passenger car intelligent suspension system. InECCE 2011 - International Conference on Electrical, Control and Computer Engineering. 2011:404–9.

[26] Hudha K, Jamaluddin H, Samin PM, Rahman RA. Effects of control techniques and damper constraint on the performance of a semi-active magnetorheological damper. International Journal of Vehicle Autonomous Systems. 2005;3:230-52.

[27] Hewit JR, Burdess JS. Fast dynamic decoupled control for robotics, using active force control. Mechanism and Machine Theory. 1981;16:535–42.

[28] Mailah M, Mun H, Kazi S, Jahanabadi H. Experimental implementation of active force control and iterative learning technique to a two-link arm driven by penumatic artificial muscles. Recent Researches in Computational Intelligence and Information Security. 2011:216–21.

[29] Mailah M, Hooi HM, Kazi S, Jahanabadi H. Practical active force control with iterative learning scheme applied to a pneumatic artificial muscle actuated robotic arm. International Journal of Mechanics. 2012;6:88–96.

[30] Mailah M, Hewit JR, Meeran S. Active Force Control Applied to a Rigid Robot Arm. Jurnal Mekanikal. 1996;2:52–68.

[31] Priyandoko G, Mailah M, Jamaluddin H. Vehicle active suspension system using skyhook adaptive neuro active force control. Mechanical Systems and Signal Processing. 2009;23:855–68.

[32] Priyandoko G, Mailah M, Jamaluddin H. Practical Implementation of Skyhook and Adaptive Active Force Control To an Automotive Suspension. 2nd Regional Conference on Vehicle Engineering & Technology. 2008:1-8.

[33] Mailah M, Priyandoko G. Mechatronic implementation of an intelligent active force. International Review of Mechanical Engineering. 2010;4:899–907.